

ARTICLE

Received 10 Dec 2014 | Accepted 24 Sep 2015 | Published 6 Nov 2015

DOI: 10.1038/ncomms9717

Cytokinin response factors regulate *PIN-FORMED* auxin transporters

Mária Šimášková^{1,2}, José Antonio O'Brien^{1,2}, Mamoon Khan³, Giel Van Noorden^{1,2}, Krisztina Ötvös³, Anne Vieten⁴, Inge De Clercq^{1,2}, Johanna Maria Adriana Van Haperen⁵, Candela Cuesta³, Klára Hoyerová⁶, Steffen Vanneste^{1,2}, Peter Marhavý³, Krzysztof Wabnick³, Frank Van Breusegem^{1,2}, Moritz Nowack^{1,2}, Angus Murphy⁷, Jiří Friml³, Dolf Weijers⁵, Tom Beeckman^{1,2} & Eva Benková³

Auxin and cytokinin are key endogenous regulators of plant development. Although cytokinin-mediated modulation of auxin distribution is a developmentally crucial hormonal interaction, its molecular basis is largely unknown. Here we show a direct regulatory link between cytokinin signalling and the auxin transport machinery uncovering a mechanistic framework for cytokinin-auxin cross-talk. We show that the CYTOKININ RESPONSE FACTORS (CRFs), transcription factors downstream of cytokinin perception, transcriptionally control genes encoding *PIN-FORMED* (*PIN*) auxin transporters at a specific *PIN* CYTOKININ RESPONSE ELEMENT (PCRE) domain. Removal of this *cis*-regulatory element effectively uncouples *PIN* transcription from the CRF-mediated cytokinin regulation and attenuates plant cytokinin sensitivity. We propose that CRFs represent a missing cross-talk component that fine-tunes auxin transport capacity downstream of cytokinin signalling to control plant development.

¹Department of Plant Systems Biology, VIB, Technologiepark 927, B-9052 Gent, Belgium. ²Department of Plant Biotechnology and Bioinformatics, Ghent University, Technologiepark 927, B-9052 Gent, Belgium. ³Institute of Science and Technology Austria (IST Austria), Am Campus 1, 3400 Klosterneuburg, Austria. ⁴Department of Developmental Genetics, Centre for Molecular Biology of Plants, University Tübingen, Auf der Morgenstelle 3, 72076 Tübingen, Germany. ⁵Laboratory of Biochemistry, Wageningen University, Dreijenlaan 3, 6703HA Wageningen, the Netherlands. ⁶Institute of Experimental Botany, ASCR, Rozvojová 263, 16502 Prague, Czech Republic. ⁷Department of Plant Science and Landscape Architecture, University of Maryland, College Park, Maryland 20742, USA. Correspondence and requests for materials should be addressed to E.B. (email: eva.benkova@ist.ac.at).

The hormones auxin and cytokinin are essential to control plant growth and development including early embryogenesis^{1,2} and postembryonic organogenic processes, such as root^{3–5} and shoot⁶ branching, phyllotaxis⁷, shoot^{8,9} and root apical meristem activity^{10,11} and vascular development^{12,13}. The principal pathways that manage their metabolism, distribution, and perception and the backbone molecular components have been identified^{14–17}. Importantly, a complex network of interactions and feedback circuits interconnects both pathways and determines the final outcome of the individual hormone actions. Well-established are the mutual regulation of metabolic¹⁸ and signalling pathways^{2,8}, as well as the cytokinin-mediated modulation of auxin transport^{10–12}. Cytokinin has been shown to influence cell-to-cell auxin transport by modification of the expression of several auxin transport components and thus to modulate auxin distribution important for root development^{10,11,19,20}. Through the cytokinin receptor ARABIDOPSIS HISTIDINE KINASE3 (AHK3) and the downstream signalling components ARABIDOPSIS RESPONSE REGULATOR (ARR1) and ARR12, cytokinin has been shown to activate SHY2/IAA3 (SHY2), a repressor of auxin signalling that negatively regulates the PIN auxin transporters¹⁰. However, thus far, the components of the transcriptional complex that directly control *PIN* transcription in response to cytokinin are unknown.

Here we show that the cytokinin response factors (CRFs)²¹ transcriptionally control *PIN-FORMED* (*PIN*) genes encoding auxin transporters at a specific *PIN* CYTOKININ RESPONSE ELEMENT (*PCRE*) domain. Removal of this *cis*-regulatory element effectively uncouples *PIN* transcription from the CRF-dependent regulation and attenuates plant cytokinin sensitivity. Accordingly, plants with modified CRF activity exhibit alterations in the expression of *PIN* genes and developmental defects mimicking phenotypes of auxin distribution mutants. We propose that the CRFs act as components of the transcriptional regulatory complex, which mediates transcriptional control downstream of cytokinin and fine-tunes *PIN* expression during plant growth and development.

Results

The *PCRE* element mediates cytokinin-sensitive *PIN7* expression.

To explore the upstream pathway mediating cytokinin-dependent *PIN* transcription, we searched for regulatory elements by a promoter-deletion analysis of the *PIN7* and *PIN1* promoters (Supplementary Fig. 1a). Initially, we focused on *PIN7* of which transcription has previously been shown to be activated by cytokinin^{11,12}. We confirmed that the promoter (1,423 bp upstream of the translational start site) of *PIN7* fused to the *green fluorescent protein* (*GFP*) reporter gene (Supplementary Fig. 1a) is activated by cytokinin and that this region is sufficient to mediate the hormonal response (Fig. 1a). The abrupt change in the cytokinin response as a consequence of a 200-bp element deletion between 1,423 and 1,223 bp upstream of the *ATG* start codon hinted at the presence of a *cis*-regulatory element required for the cytokinin-mediated transcriptional control of *PIN7* (Fig. 1b). The role of this regulatory element, designated as *PCRE7*, in cytokinin-sensitive expression was further tested with a *PIN7-GFP* translational construct driven by the truncated Δ *PIN7* promoter. Quantification of the membrane *PIN7-GFP* signal demonstrated that the expression, when driven by the truncated promoter, was largely insensitive to cytokinin treatment in the cells of the central root cylinder (Fig. 1c–e), as well as in the initials of lateral root primordial (LRP) (Supplementary Fig. 2a–e). The Δ *PIN7* promoter activity was significantly weakened in the root provascular and columella cells when compared with the full *PIN7* promoter, indicating the importance of this promoter element for the

regulation of the *PIN7* steady-state expression (Fig. 1a,c compared with Fig. 1b,d and e). Hence, the loss of cytokinin sensitivity as a consequence of the promoter truncation implies the presence of a specific *cis*-regulatory element on which the cytokinin-susceptible transcriptional complex might act to fine-tune *PIN7* expression in response to cytokinin. While the reason for the change in steady-state expression levels remains to be determined, based on the overlap between *PIN7* expression and that of the *TCS::GFP* cytokinin-responsive reporter in procambial cells¹², we propose that cytokinin might, through this regulatory element, participate not only in the response to exogenously applied cytokinin but also in the establishment and maintenance of proper basal levels of *PIN7* expression.

Truncation of the *PIN7* promoter disrupts plant growth.

Cytokinin-regulated plant growth and development has been proposed to be partly mediated by cytokinin-controlled *PIN* expression^{10,11}. To dissect the developmental role of cytokinin-regulated *PIN* expression, plants expressing *PIN7-GFP* under the control of the truncated cytokinin-insensitive Δ *PIN7* promoter or the wild-type *PIN7* promoter were crossed with the *pin7* mutant background and their seedlings were thoroughly inspected. Root growth analyses revealed that in young seedlings (7-day-old), growth of roots expressing either *PIN7::PIN7-GFP/pin7* or Δ *PIN7::PIN7-GFP/pin7* was indistinguishable. In contrast, 14-day-old Δ *PIN7::PIN7-GFP/pin7* roots were significantly longer than control *PIN7::PIN7-GFP/pin7* roots (Fig. 1f,h). Furthermore, truncation of the *PIN7* promoter strongly interfered with the cytokinin sensitivity of root growth (Fig. 1g,h), root meristem size (Fig. 1i), lateral root initiation and development (Fig. 1g,j). Some phenotype features, such as primary root growth and its resistance to cytokinin, were comparable to the *pin7* phenotype. However, reduced sensitivity of the root meristem as well as of the lateral root initiation to cytokinin were more pronounced in Δ *PIN7::PIN7-GFP/pin7* seedlings.

While we cannot exclude that these phenotypes are influenced by a change in the basal expression levels of *PIN7*, on the basis of the altered cytokinin sensitivity of the transgenics, we suggest that regulation of *PIN7* by cytokinins via *PCRE7* is required for proper root growth and development.

CRFs control *PIN7* transcription. To identify the upstream regulatory factors that control *PIN7* transcription by direct interaction with *PCRE7*, we employed a yeast one-hybrid (Y1H) assay. We screened the REGIA open reading frame (ORF) library that contains a set of ~1,300 *Arabidopsis* transcription factors (TFs) and transcriptional regulators²². The Y1H screen with *PCRE7* as bait (Supplementary Fig. 3a), identified CRF2, CRF3, and CRF6 that belong to the cytokinin-inducible subset of the APETALA2 (AP2)/ETHYLENE RESPONSIVE FACTOR family of TFs²¹ (Fig. 2a). To confirm that the CRFs physically interact with *PCRE7*, we analysed the *CRF2::CRF2-GFP* and *35S::CRF6-GFP* transgenic plants through chromatin immunoprecipitation (ChIP) followed by quantitative PCR assays (ChIP-qPCR). Chromatin immunoprecipitated with anti-GFP antibodies was profoundly enriched in the *PCRE7* region. No enrichment was detected when other distant sequences in the *PIN7* (*PIN7* (-553–357)) promoter were tested (Fig. 2c,d; Supplementary Fig. 1c). Hence, CRFs are directly associated with the *PCRE7*.

To gain insight into the role of the CRFs in the regulation of *PIN* transcription, we performed a transient expression assay in *Arabidopsis* protoplasts. The expression of the *PIN7::LUCIFERASE* (*LUC*) reporter was strongly activated when co-expressed with *CRF2* and *CRF6* (Fig. 2e,f), but not with *CRF3* driven by

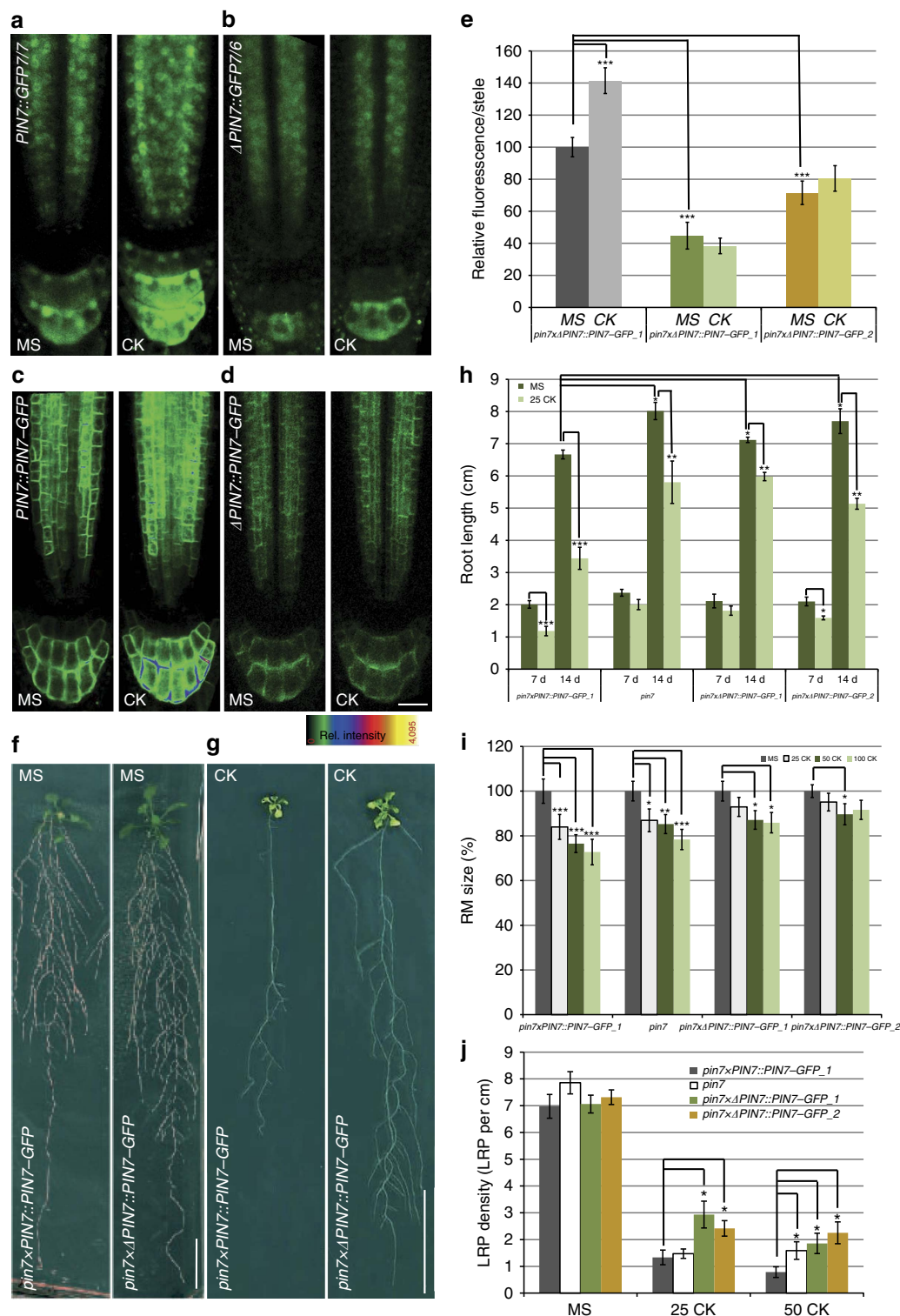


Figure 1 | Truncation of *PIN7* promoter results in cytokinin-insensitive *PIN7* transcription. (a–e) Expression of GFP (a,b) and *PIN7*-GFP (c,d) is upregulated in response to cytokinin when driven by the full *PIN7* (a,c), but not the truncated Δ *PIN7* (b,d) promoter. Green: nuclear-localized GFP (a,b); membrane-localized *PIN7*-GFP (c,d). A semi-quantitative colour-coded heat map of the GFP fluorescence intensity is provided. Quantification of *PIN7*-GFP in the provascular tissue of primary roots (e). Roots of 7-day-old seedlings ($n=15$) were treated with control Murashige and Skoog (MS) medium with or without 5 μ M of the cytokinin (CK) N6-benzyladenine for 8 h. Student's t -test (*** $P<0.001$, $n=15$). (f–j) Seedlings expressing Δ *PIN7::PIN7-GFP* in the *pin7* background exhibit enhanced root growth (f,h) and reduced cytokinin sensitivity of primary root growth (f–h), root meristem (RM) size (i) and lateral root initiation (j). Seedlings were grown for 28 (f,g), 14 (h) and 7 days (d) (h–j) on MS medium with or without following cytokinins: 0.025 μ M N6-benzyladenine (f–h); 0.025, 0.05 and 0.1 μ M N6-benzyladenine (i); and 0.025 and 0.05 μ M N6-benzyladenine (j). Student's t -test (* $P<0.05$; ** $P<0.01$; *** $P<0.001$ (h,j); or * $P<0.01$; ** $P<0.001$; *** $P<0.0001$ (i); $n=10$ –15). Δ *PIN7::PIN7-GFP_1* and Δ *PIN7::PIN7-GFP_2* represent two independent transgenic lines crossed into the *pin7* mutant background. Error bars represent s.e. Scale bars, 20 μ m (a–d), 2 cm (f–g). Results were reproducible in three independent experiments.

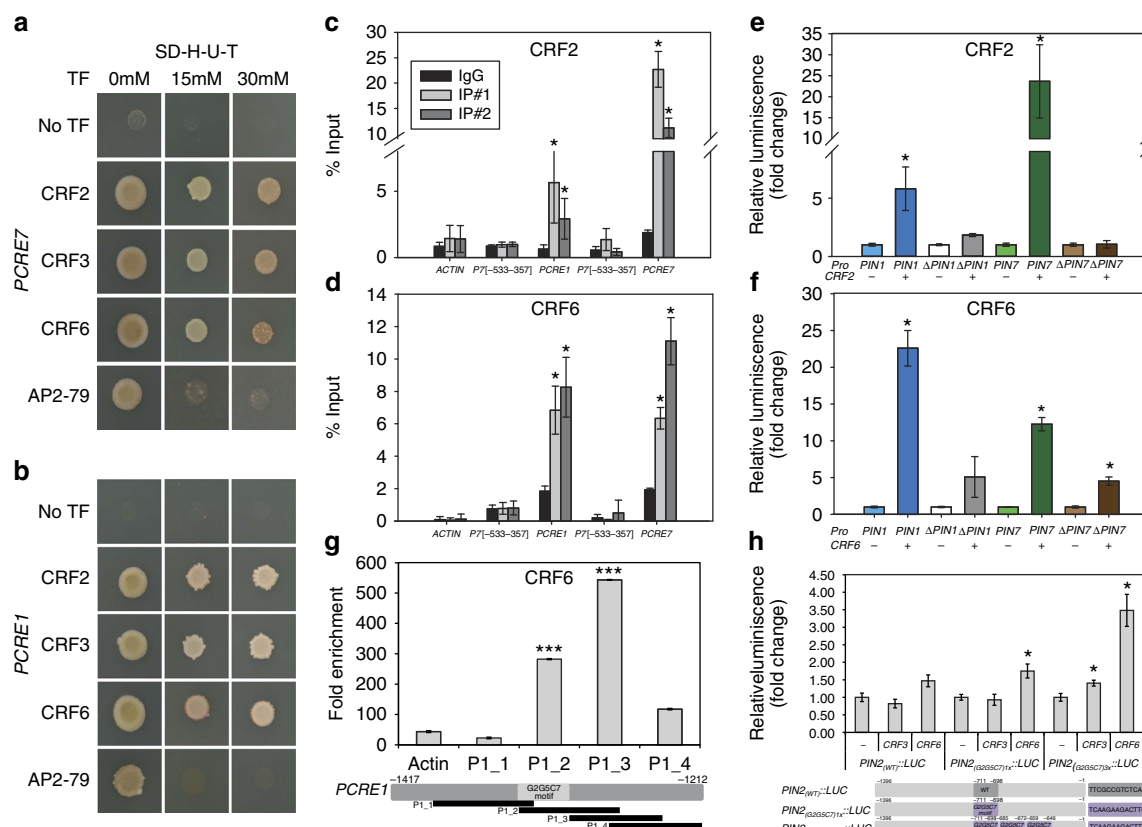


Figure 2 | Cytokinin response factors interact with PCREs. (a,b) CRF2, CRF3 and CRF6 interaction with *PCRE7* (a) and *PCRE1* (b) results in HIS3 reporter activation in an Y1H assay in contrast to AP2-79 that does not interact. Yeast cells were grown on SD-H-U-T minimal media without histidin (H), uracil (U) and tryptophan (T), supplemented with 3-amino-1,2,4-triazole (3AT). (c,d) Interaction of CRF2 (c) and CRF6 (d) with *PCRE1* and *PCRE7* detected by chromatin immunoprecipitation (ChIP). Chromatin immunoprecipitated with anti-GFP antibody is enriched in the *PCRE1* and *PCRE7* region. No enrichment was detected with *PIN7* (-553-357) and *PIN1* (-512-433) elements. (e,f) Significantly upregulated expression of *PIN1::LUC* and *PIN7::LUC*, by co-expression with CRF2 (e) and CRF6 (f) in contrast to their truncated counterparts (Δ *PIN1::LUC*, Δ *PIN7::LUC*) in *Arabidopsis* mesophyll protoplasts, Student's t-test (* P < 0.01, n = 3). (g) ChIP of CRF6-GFP reveals a significantly higher enrichment for regions either containing (P1_2) or directly neighbouring (P1_3) the 5'-AGCAGAC-3' motif when compared with more distant regions in *PCRE1* (P1_1 and P1_4) (** P < 0.0001, n = 3) (h). CRF6 increases expression of *PIN2* promoter containing three G2G5C7 motifs in *Arabidopsis* root cell suspension protoplasts (* P < 0.01, n = 5) (h). Error bars represent s.e. (protoplast assay) and s.d. (ChIP). Experiments were repeated at least three times.

constitutive 35S promoter (Supplementary Fig. 3b). Noteworthy, when co-expressed, CRF3 significantly attenuated the positive effect of CRF6 on *PIN7::LUC* expression (Supplementary Fig. 3c), indicating that individual CRFs might regulate *PIN7* transcription differentially. No increase in the *LUC* reporter expression was detected when CRF2 was co-expressed with the truncated Δ *PIN7::LUC* construct (Fig. 2e). Co-expression with CRF6 stimulated Δ *PIN7::LUC* expression, but less when compared with the effect on the *PIN7::LUC* (Fig. 2f) thus further confirming the importance of the *PCRE7* for CRF-dependent transcription. Collectively these data demonstrate that CRFs contribute to the transcriptional control of the *PIN7* gene through physical interaction with a specific domain in its promoter.

CRFs regulate transcription of *PIN1* auxin efflux carrier. Next we examined whether other *PIN* family members are transcriptionally controlled by CRFs similarly to *PIN7*. Using promoter deletion analysis, we found that removal of the 200 bp between 1,417 and 1,212 bp upstream of the ATG codon resulted in cytokinin insensitivity of *PIN1* transcription, hinting at the presence of the *PCRE1* cis-regulatory element mediating cytokinin-induced transcriptional control in the *PIN1* promoter (Supplementary Figs 1b and 4a–e). An Y1H assay confirmed an

interaction of CRF2, CRF3 and CRF6 with this element (Fig. 2b; Supplementary Fig. 3a). Accordingly, chromatin immunoprecipitated with anti-GFP antibodies from *CRF2::CRF2-GFP* and *35S::CRF6-GFP* transgenic plants was profoundly enriched in the *PCRE1*, while no enrichment was detected for distant sequence in the *PIN1* promoter (*PIN1* (-512-433)) (Fig. 2c,d). The expression of *PIN1::LUC*, but not of Δ *PIN1::LUC*, was strongly activated when transiently co-expressed with CRF2 and CRF6, in protoplasts (Fig. 2e,f). Similar to *PIN7*, CRF3 did not significantly affect *PIN1::LUC* expression, but attenuated the CRF6-stimulatory effect when co-expressed (Supplementary Fig. 3d,e). Altogether, these results indicate that *PIN1* and *PIN7* share common upstream regulatory components controlling their expression in response to cytokinin.

***PCRE1* and *PCRE7* contain motifs recognized by CRFs.** Alignment of *PCRE1* and *PCRE7* elements with the Align programme (based on the ClustalW algorithm)²³ displayed a 54% sequence identity, suggesting that the cytokinin-dependent regulation of *PIN1* and *PIN7* might be governed by TFs recognizing common types of regulatory motifs. Previously, the GCC box (5'-AGCCGCC-3') has been proposed as a binding motif recognized by ETHYLENE RESPONSE

FACTOR1 (ERF1), a TF of the AP2/ERF family^{21,24}, including CRF2, CRF3 and CRF4 (ref. 25). Scanning of *PIN1* and *PIN7* promoters revealed that neither *PCRE1* nor *PCRE7* contains a GCC box, and there is one GCC box located at (−483 bp) upstream of ATG in the *PIN1* promoter (Supplementary Fig. 1d). However, no significant enrichment for the *PIN1* fragment (−512–433) which contains this motif was detected using the ChIP–qPCR assay, indicating that CRF2 and CRF6 do not exhibit an increased affinity to this binding site (Fig. 2c,d). Noteworthy, several studies demonstrated that nucleotides G2, G5 and C7 at conserved positions might be essential for the recognition of the GCC-derived motif by TFs of the AP2/ERF family²⁶. We found that *PCRE1* and *PCRE7* contain 5′-AGCAGAC-3′ and 5′-AGAAGAC-3′ motifs, respectively, with critical nucleotides at conserved positions (Fig. 2g; Supplementary Fig. 1c,d). To examine the relevance of these motifs for CRF binding, we tested whether CRF6 associates with them by ChIP–qPCR. Using specific primer combinations, we inspected enrichment for the short fragments spanning *PCRE1* (ref. 27). Significantly increased enrichment detected for fragments either containing or directly neighbouring the 5′-AGCAGAC-3′ site when compared with more distant fragments in *PCRE1*, strongly supports this motif as a CRFs’ recognition site (Fig. 2g). Additional thorough scanning for the presence of G2, G5 and C7 motifs revealed one more motif in both *PIN1*, as well as *PIN7* promoters (Supplementary Fig. 1c,d).

To further support our conclusion on the CRF-mediated regulation of *PIN* expression, we tested whether the *PIN2* promoter, previously found to be cytokinin insensitive²⁸ might be activated by CRF after introducing the 5′-AGAAGAC-3′ motif. Detailed scanning of the *PIN2* promoter sequence revealed that there are no 5′-AGCAGAC-3′ and 5′-AGAAGAC-3′ motifs present in the *PIN2* promoter sequence within 2,500 bp upstream of the translation start and there is one 5′-GCCGTC-3 motif located at (−698 bp) upstream of the translational start. When the *PIN2::LUC* reporter was co-expressed with CRF6, a 1.47 ± 0.38 -fold increase of *LUC* activity (\pm indicates s.e., $n=5$) was detected, indicating modest CRF6 activity for the regulation of *PIN2* promoter (Fig. 2h). Replacement of the 5′-GCCGTC-3′ motif in the *PIN2* promoter by either one or three copies of the 5′-AGAAGAC-3′ motif resulted in a 1.75 ± 0.17 - and 3.48 ± 1.02 -fold increase of the *LUC* activity, respectively (Fig. 2h; \pm indicates s.e., $n=5$). Hence, insertion of the 5′-AGAAGAC-3′ motif in triplicate into the *PIN2* promoter significantly increased sensitivity to CRF6 (Fig. 2h), thus corroborating relevance of the motif identified in the *PCRE7* element for CRF6-mediated expression. In line with previous observations, no dramatic effect on *PIN2*, as well as on the *PIN2* promoter containing *PCRE7* motifs could be detected when co-expressed with CRF3 (Fig. 2h).

Previously, type-B ARR have been proposed to mediate cytokinin regulation of *PIN1* and *PIN7* expression through direct transcriptional control of the *IAA3/SHY2* repressor of auxin signalling¹⁰. Three type-B ARRs (ARR10, ARR11 and ARR14) tested in an Y1H assay did not exhibit interaction with either *PCRE1* or *PCRE7*, which indicates that cytokinin transcriptional regulation of *PIN1* and *PIN7* might not occur by their direct binding to *PCREs* (Supplementary Fig. 3f).

Altogether, these data suggest that CRF2 and CRF6 might recognize specific motifs within *PCRE1* and *PCRE7* with G2, G5 and C7 at conserved positions to control *PIN1* and *PIN7* expression.

Expression of *PIN7* and *PIN1* is altered in *crf* mutants. The initial expression analysis revealed that the expression

patterns of CRFs, and *PIN1* and *PIN7* largely overlap in roots²⁹ (Supplementary Fig. 5 compared with Fig. 1a and Supplementary Fig. 4a,c), supporting their role as direct transcriptional regulators. To evaluate the impact of CRFs on *PIN7* and *PIN1* expression *in planta*, we examined lines with a modulated activity of CRFs (Supplementary Fig. 6). Analyses of *PIN7* expression using quantitative reverse transcription–PCR (qRT–PCR), as well as monitoring of *PIN7::PIN7–GFP*, *PIN7::GUS*, *PIN7::GFP* and *PIN7::PIN7–GUS* reporters revealed a significant increase of *PIN7* expression in the root provasculture of *RPS::CRF2* and *35S::CRF6*, but not of *35S::CRF3* lines (Fig. 3a,b,e and Supplementary Fig. 7a–j). This is largely in agreement with the results of a transient protoplast assay (Fig. 2e,f compared with Fig. 3a,b,e). Lack of the *PCRE7* in the Δ *PIN7::PIN7–GFP* line interfered with the stimulatory effect of CRF2 on *PIN7–GFP* expression, regardless of cytokinin levels (Fig. 3c,d). Analysis of *PIN7* expression using *PIN7::PIN7–GFP* and *PIN7::GUS* reporters, as well as qRT–PCR in mutants lacking either of the CRFs revealed attenuated *PIN7* expression in *crf3*, as well as *crf2crf3crf6* roots and enhanced *PIN7* expression in *crf6* roots (Supplementary Fig. 7k–s).

Similar to *PIN7*, *PIN1* expression was significantly upregulated in roots overexpressing CRF2 as detected by using *PIN1::PIN1–GFP* and *PIN1::GFP* reporters, as well as by qRT–PCR. Deletion of the *PCRE1* in the Δ *PIN1::PIN1–GFP* line interfered with the stimulatory effect of CRF2 on *PIN1* expression in agreement with the proposed role of the *PCRE1* in CRF-dependent transcriptional control (Supplementary Fig. 8a–d).

Inspection of *crf* loss-of-function mutants further confirmed the role of CRFs in the regulation of *PIN1* expression *in planta*. *PIN1* expression was significantly reduced in *crf2*, *crf3*, *crf3crf6* and *crf2crf3crf6* loss-of-function mutants (Supplementary Fig. 8e–g), thus resembling the *PIN7* expression pattern in these mutant backgrounds.

Altogether, the expression analysis data support a role of the CRFs in balancing the *PIN7* and *PIN1* transcription. Nevertheless, inconsistency in *PIN7* and *PIN1* expression patterns observed in lines with modulated CRF expression, such as downregulation of both *PIN1* and *PIN7* in *crf3*, and upregulation in *crf6*, might reflect the presence of intricate *in planta* regulatory mechanisms, for example, the existence of a transcriptional complex in which additional components could function as modifiers. This is strongly supported by recent observations that individual CRFs might interact with other family members, as well as with type-B ARRs³⁰. Collectively, our data demonstrate that CRFs contribute to balancing *PIN7* and *PIN1* expression and that CRF homologues might have specific functions in the control of *PIN* expression.

CRFs mutants display an auxin transport-defective phenotype.

To examine a role of CRFs as direct upstream regulators of *PIN* transcription, we analysed in detail the phenotype of plants with modulated CRF expression. Altered expression of *PINs* in *crf* loss-of-function mutants might result in an abnormal auxin distribution and, consequently, in developmental and patterning defects as previously demonstrated for auxin distribution mutants^{1,31}. Indeed, auxin measurements in root tips of *crf3crf6* mutants revealed an increase in auxin levels (Fig. 4a). Similarly, the auxin accumulation at root tips of a mutant lacking *PIN4* auxin efflux carrier activity has been previously observed³¹.

By closer examination of plants lacking CRF activity, developmental abnormalities were found reminiscent of those caused by impaired auxin transport. A significantly enhanced number of embryonic defects, such as abnormal divisions of upper suspensor cells and in the embryo proper, and occasionally

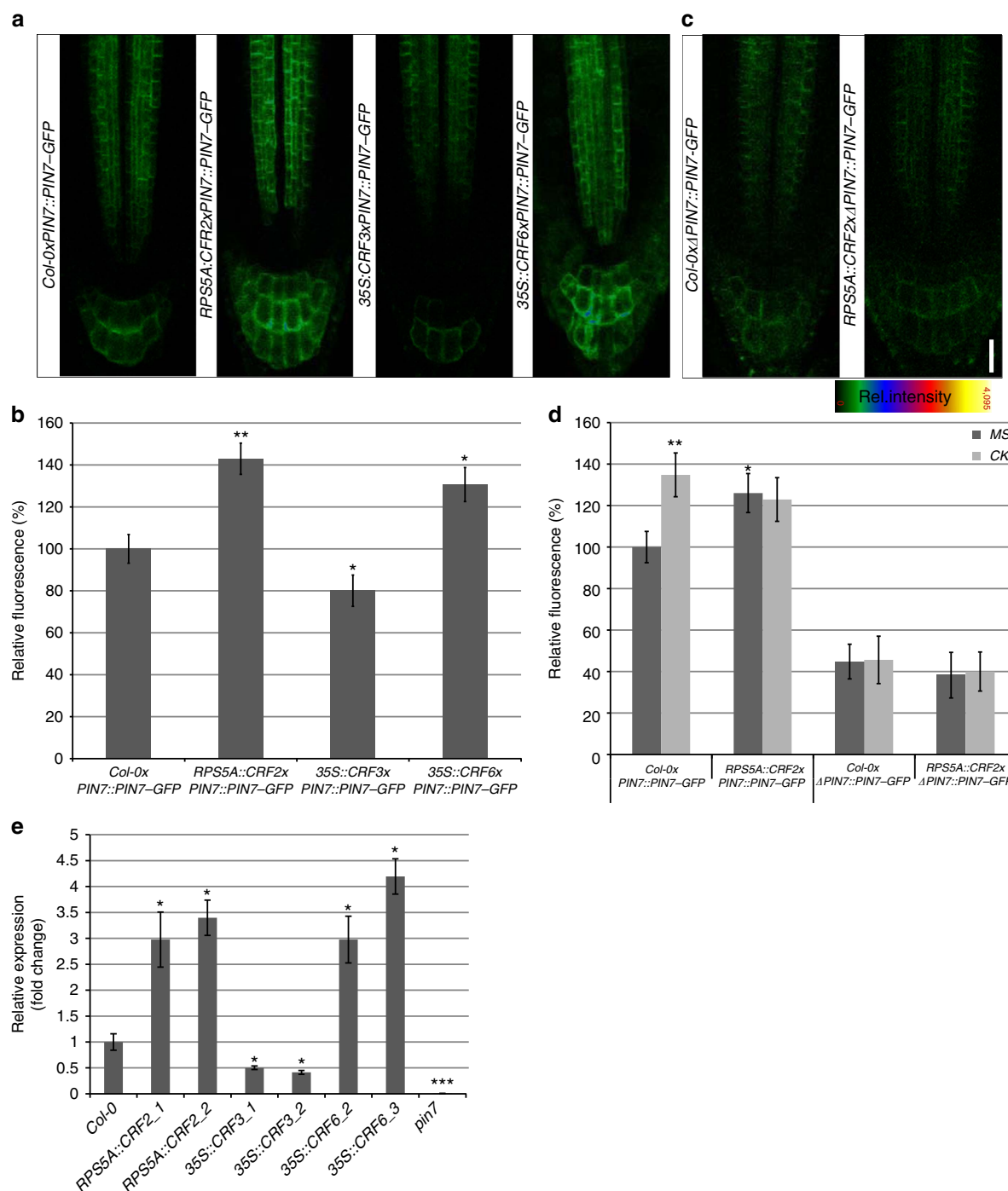
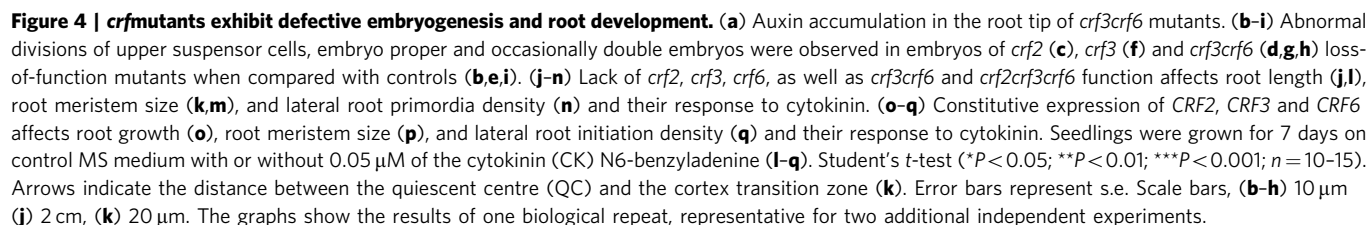


Figure 3 | Expression of *PIN* genes is altered in *CRF*-overexpressing lines. (a,b) *PIN7::PIN7-GFP* expression is upregulated in the provascular of *CRF2* and *CRF6*, but downregulated in *CRF3*-overexpressing lines. **(c,d)** Δ *PIN7::PIN7-GFP* is not upregulated in the *CRF2*-overexpressing line in either absence or presence of cytokinin (5 μ M N6-benzyladenine for 5 h). The membrane *PIN7-GFP* signal was quantified in the pericycle **(b,d)**. Student's *t*-test (**P* < 0.05, ***P* < 0.01; *n* = 15–20). **(e)** *PIN7* expression in lines overexpressing *CRFs* monitored by qRT-PCR, no expression detected in *pin7* mutant (**P* < 0.05; ****P* < 0.0001, *n* = 3). Error bars represent s.e. Seven-day-old seedlings were analysed. Scale bar, 20 μ m. Three independent experiments were performed giving the same statistically significant results.

the appearance of double embryos, was observed in embryos of *crf2*, *crf3* and *crf3crf6* loss-of-function mutants when compared with control lines (Fig. 4b–i), thus phenocopying the *pin1*, *pin7* and multiple *pin* embryo defects¹. Accordingly, *CRF2*, *CRF3* and *CRF6* expression was detected in early embryos (Supplementary Fig. 5). Lack of functional *CRF2*, *CRF3*, both *CRF3* and *CRF6* or *CRF2*, *CRF3*, *CRF6* correlated with reductions in root length, root meristem size and lateral root

initiation (Fig. 4j–n), which are developmental aberrations typically associated with defective auxin transport^{3,32,33}. On the contrary, *crf6* loss-of-function mutants, in which *PIN7* expression was enhanced, exhibited longer roots and a larger root meristem (Fig. 4j–n). Altogether, modulation of *CRF* activity alters auxin accumulation in the root tips, and leads to developmental defects in many aspects, mimicking phenotypes of auxin distribution mutants^{1,31,32}.



CRFs fine-tune root system response to cytokinin and auxin.

Typically, an increase in cytokinin activity alters root growth and development: cytokinins restrict root elongation growth, cause shortening of the root meristem size, and compromise the initiation and development of the lateral roots^{4,5,10,11,34,35}. While cytokinin inhibitory effects of root elongation involves ethylene^{11,34}, reduction of the root meristem size, as well as lateral root initiation by cytokinin occurs largely in an ethylene independent manner^{5,11}. To examine the possible role of CRFs in cytokinin-mediated root system establishment, lines with modulated CRF activity were exposed to increased cytokinin concentrations. We found that neither gain nor loss of CRF activity dramatically changed root growth response to cytokinin (Fig. 4l,o). The root meristem cytokinin response was unaffected in *crf2* and *crf6* mutants and reduced in *crf3* and *crf3crf6*, as well as *crf2crf3crf6* mutants (Fig. 4m). Constitutive expression of *CRF2*, *CRF3* and *CRF6* reduced root meristem response to cytokinin (Fig. 4p). Noteworthy, most pronounced changes were observed in cytokinin effect on lateral root initiation and development. The significant increase in cytokinin inhibitory effects on both lateral root initiation and development was detected in *crf3*, *crf3crf6* and *crf2crf3crf6* mutants (Fig. 4n; Supplementary Fig. 9a–e), whereas *CRF2* and *CRF6* overexpression attenuated cytokinin effects (Fig. 4q; Supplementary Fig. 9f,g). In contrast to cytokinin, root system response to auxin was reduced in *crf3*, *crf3crf6* and *crf2crf3crf6* mutants, which was manifested by an attenuated stimulatory effect of auxin on lateral root initiation (Supplementary Fig. 10a–e). Constitutive expression of *CRF2* led to significantly enhanced response to auxin, whereas no dramatic changes in lateral root initiation after auxin treatment in either the *CRF3* or *CRF6* overexpressor line when compared with the wild-type control were detected (Supplementary Fig. 10f–h). Hence, perturbations in *CRF* expression affect root response to cytokinin and auxin, and indicate that CRFs by control of auxin transport might fine-tune cytokinin- and auxin-mediated root growth and development.

Discussion

Auxin gradients represent universal mechanisms to control plant organogenesis. Modulation of the activity of the transport machinery that regulates auxin distribution directly impacts on organ formation and patterning and, thus, accounts for a developmentally efficient tool to flexibly adapt plant architecture depending on the changing environmental conditions. Recently, evidence accumulates that exogenous factors, such as light or gravity, through their endogenous counterpart, that is, plant hormones including ethylene, gibberellin, jasmonate and cytokinin, modulate the activity of the polar auxin transport machinery to direct plant growth and development^{10,11,19,36–39}. However, the molecular basis of these regulations are scarcely understood so far.

Here we demonstrate that the expression of auxin efflux transporters can be effectively uncoupled from cytokinin control through deletion of the *PCRE* cis-regulatory element in the promoter of the *PIN* auxin efflux carrier gene. Moreover, we found that the activity of the Δ *PIN7* promoter lacking *PCRE7* was significantly reduced in the root provascular and in columella cells when compared with the full *PIN7* promoter, indicating the importance of this promoter element for the regulation of basal *PIN7* expression and it suggests that cytokinin might participate in the establishment and maintenance of the proper expression level of *PIN7* through this regulatory element. Truncation of the *PIN7* promoter causes loss of cytokinin-dependent *PIN7* transcription and impacts on cytokinin-mediated root growth and branching. While it is difficult to conclusively attribute these phenotypes directly to the loss of cytokinin sensitivity as opposed to a change in basal expression levels, the altered

cytokinin responsiveness of the transgenic plants suggests, that tightly controlled *PIN*-dependent auxin transport may be significant in the establishment of the root system architecture.

Attempts to reveal components of the upstream regulatory pathway acting at the *PCRE* led to the identification of CRFs as direct transcriptional regulators. Originally, CRFs have been found as a subgroup of the AP2 family of TFs, which are rapidly induced by cytokinin, and they have been proposed to mediate the transcriptional response to cytokinin²¹. However, the CRFs' downstream targets and pathways remained unknown so far. Here we show that through interaction with the cis-regulatory *PCRE*, presumably through recognition of the 5'-AGCAGAC-3'-like motif, CRFs control expression of *PIN1* and *PIN7*.

Interestingly, although *PIN7* and *PIN1* share common molecular components mediating transcriptional regulation by cytokinin, the expression of *PIN7* is upregulated, whereas expression of *PIN1* is downregulated in response to exogenous cytokinin. The finding that *PIN* transcription is differentially controlled by individual CRFs, for example, *CRF3* counteracts both *CRF2*- as well as *CRF6*-stimulatory effects, indicates that the final output might depend on the balance between individual CRFs and their mutual interactions³⁰ in certain tissues. It is also possible that the transcriptional activity of individual CRFs can be attenuated by additional molecular modifiers.

Modulation of the CRF activity results in significant changes of the *PIN1* and *PIN7* expression patterns and in phenotype aberrations reminiscent of mutants with defective auxin transport^{1,31,32}. This, together with a significant overlap in the expression of *PIN* and *CRF* genes during embryogenesis, in the root meristems and LRP, strongly supports a role of CRFs in the regulation of *PIN* expression. Accordingly, the expression of several CRFs in vascular tissue has been correlated with alterations of the vascular patterning in *CRF* loss-of-function mutants⁴⁰, similarly to those observed in auxin transport mutants⁴¹.

In this light, the identification of the *PIN* genes as direct targets of CRFs reveals a missing direct regulatory link between the cytokinin signalling and the auxin transport machinery. Moreover, *CRF2* (*TARGET OF MONOPTEROS* (*TMO3*)) as a direct transcriptional target of the *AUXIN RESPONSE FACTOR5/MONOPTEROS*⁴² might account for an important convergence point to the previously characterized *AHK3-ARR*, *ARR12-IAA3/SHY2* regulatory chain¹⁰ and balance both auxin and cytokinin input to control auxin transport. Furthermore, the recent observation that *CRF6* is induced by numerous stresses²⁹ hints at a role of CRFs as factors modulating auxin transport in response to environmental signals.

Methods

Plant material and growth conditions. The transgenic *Arabidopsis thaliana* (*L.*) *Heynh.* lines have been described elsewhere: *PIN1::PIN1-GFP³*, *pin7-2* (ref. 3), *PIN7::PIN7-GFP³²*, *PIN7::GUS¹*, *RP55A::CRF2* (ref. 42), *35S::EGFP-CRF6* (ref. 43). The previously characterized *CRF* knockout mutants²¹ were obtained from various T-DNA insertion mutant seed collections: *crf2-1*, *crf2-2*, *crf3-1* and *crf3-2* from the Salk Institute Genomic Analysis Laboratory (SAIL, former GARLIC) T-DNA insertion lines from the Torrey Mesa Research Institute⁴⁴ and *crf6-S2* and *crf6-11.2* from GABI-Kat⁴⁵. The *crf3crf6* double and *crf2crf3crf6* triple mutants were generated from *crf3-1*, *crf6-S2* and *crf2-2*, and *crf3-1* and *crf6-S2* respectively. Primers and T-DNA accession numbers are listed in Supplementary Table 1. Seeds of *Arabidopsis* (accession Columbia-0) were plated and grown on square plates with solid half-strength Murashige and Skoog (MS) medium supplemented with 0.5 g l⁻¹ MES, 10 g l⁻¹ Suc and 0.8% agar. The plates were incubated at 4 °C for 48 h to synchronize seed germination and then grown vertically in growth chambers under a 16:8 h day/night cycle photoperiod at 18 °C. Cytokinin treatments were performed with the N6-benzyladenine cytokinin derivative, concentrations were adapted to the experimental setups. Typically, to examine root growth response to cytokinin, low 0.25, 0.5 and 0.1 μ M cytokinin concentrations were applied. The cytokinin impact on *PIN* expression was examined 8 h after treatment with cytokinin, therefore higher concentrations of 2 and 5 μ M were applied.

Cloning and generation of transgenic lines. For promoter analysis of *PIN1* and *PIN7*, particular promoter fragments were amplified by PCR and cloned into the *pGEM-T* vector. The used primers contained unique restriction sites: PstI-sense and BamHI-antisense for *PIN1*, and SalI-sense and BamHI-antisense for *PIN7*, allowing digestion and subsequent cloning into the *pGREEN* binary vector. The resulting constructs contained transcriptional fusions between the *PIN1* or *PIN7* promoter variants and the enhanced GFP with a nuclear localization signal (NLS). Primers used for cloning are listed in Supplementary Table 2. The translational fusion $\Delta PIN1::PIN1-GFP$ was obtained by modifying *PIN1::PIN1-GFP* (in *pBINPLUS* vector backbone³) as follows: the *PIN1* promoter sequence from -258 to -2,320 relative to the initiating ATG was removed by XbaI digestion and replaced by the *PIN1* promoter sequence spanning the -258 to -1,212 region. $\Delta PIN7::PIN7-GFP$ was derived from *PIN7::PIN7-GFP* in *pBINPLUS*¹ by removal of the EcoRI fragment. The truncated promoter construct contained 1,141 bp upstream of the translational start site. Expression plasmids were generated by standard molecular biology protocols and Gateway technology (Invitrogen). ORFs were amplified from a complementary DNA (cDNA) template with Pfu DNA Polymerase (Promega, Madison, WI, USA) and fused to the Gateway attB sites by PCR. *pDONR221* and *p4-p1r* were used as ENTRY vectors. The structure and sequence of all destination vectors were as described^{46,47} and are available online at <http://www.psb.ugent.be/gateway/> or otherwise referenced. *35S::CRF3* and *35S::CRF6* were obtained by cloning the ORFs of *CRF3* and of *CRF6* into destination vectors *pK7WG2.0* and *pK7WG2D*, respectively. Overexpression of these lines was confirmed by qPCR, primers are included in Supplementary Table 2. The *CRF3* and *CRF6* (2 kb) promoters were cloned in *pMK7S*NFm14GW*, generating the *ProCRF3::NLS-GFP-GUS* and *ProCRF6::NLS-GFP-GUS* constructs (transcriptional fusions between the promoters and the gene encoding the EGFP-GUS fusion protein), respectively. The *CRF2::CRF2-GFP* fusion, used for the ChIP experiments, was generated by cloning a DNA fragment consisting of the 2-kb *CRF2* proximal promoter and the *CRF2* coding sequence in frame to $3 \times$ GFP in the *pGreenIIK* vector. All transgenic plants were generated by the floral dip method⁴⁸. At least two independent transgenic lines were examined for expression pattern.

Quantitative RT-PCR. RNA was extracted with the RNeasy kit (Qiagen) from excised root tips of 7-day-old root sample. A DNase treatment with the RNase-free DNase Set (Qiagen) was carried out for 15 min at 25 °C. Poly(dT) cDNA was prepared from 1 µg of total RNA with the iScript cDNA Synthesis Kit (Biorad) and analysed on a LightCycler 480 (Roche Diagnostics) with the SYBR Green I Master kit (Roche Diagnostics) according to the manufacturer's instructions. Targets were quantified with specific primer pairs designed with the Beacon Designer 4.0 (Premier Biosoft International, Palo Alto, CA, USA). All PCRs were performed in triplicate. Expression levels were first normalized to ACTIN2 expression levels and then to the respective expression levels in the wild type. The primers used to quantify gene expression levels are listed in Supplementary Table 2.

Phenotypic analysis. For root length analysis, seedlings were photographed and root lengths were measured with ImageJ (<http://rsb.info.nih.gov/ij/>). To examine root growth kinetics, seedling growth was recorded daily during 14 days with an EOS035 Canon Rebel Xti camera. Long-term root growth observations for 28 days were performed on Petri dishes of 245 mm size. About 10–15 seedlings were processed, and 3 independent experiments were performed.

To determine root meristem size, 7-day-old seedlings ($n = 10-15$) were stained with propidium iodide ($1 \mu\text{M}$ ml⁻¹) and microscopy was performed using Zeiss LSM 510 confocal microscope. The distances between the quiescent centre and the first elongating cell were measured with ImageJ. To score LRP density, 7-day-old seedlings ($n = 10-20$) were first processed by clearing⁴⁹. In brief, seedlings were incubated in a solution containing 4% HCl and 20% methanol for 15 min at 57 °C, followed by 15 min incubation in 7% NaOH/60% ethanol at room temperature. Next, seedlings were rehydrated by successive incubations in 40, 20 and 10% ethanol for 5 min, followed by incubation (15 min up to 2 h) in a solution containing 25% glycerol and 5% ethanol. Finally, seedlings were mounted in 50% glycerol and root lengths were measured on scanned slides with ImageJ. Scoring of LRP was performed by using a DIC Olympus BX51 microscope.

Histochemical and histological analysis. To detect β -Glucuronidase (GUS) activity, 5-day-old seedlings were incubated in reaction buffer containing 0.1 M sodium phosphate buffer (pH 7), 1 mM ferricyanide, 1 mM ferrocyanide, 0.1% Triton X-100 and 1 mg ml⁻¹ X-Gluc for 1 up to 24 h in dark at 37 °C. Afterwards, chlorophyll was removing in 70% ethanol and seedlings were cleared⁴⁹ as described above. GUS expression was monitored by differential interference contrast microscopy (Olympus BX51).

Immunodetection of PIN1 expression in roots (5-day-old seedlings) and GFP reporter expression in *CRF2::GFP* transgenic embryos (harvested from siliques of ~4-week-old plants) were performed using an automated system (Intavis *in situ* pro) according to published protocol⁵⁰. Roots and embryos were fixed in either 4% paraformaldehyde or 4% paraformaldehyde and 0.1% Triton, respectively, for 1 h in vacuum at room temperature. Afterwards, seedlings were first incubated for 30–45 min in PBS (2.7 mM KCl, 137 mM NaCl, 4.3 mM Na₂HPO₄ 2H₂O and 1.47 mM KH₂PO₄, pH 7.4) containing 2% Driselase at 37 °C in a humid chamber,

and then in PBS supplemented with 3% NP40 and 20% DMSO for 1 h at room temperature. After blocking with 3% BSA in PBS (3 h at 37 °C), samples were incubated with primary antibody (affinity-purified rabbit anti-yellow fluorescent protein polyclonal serum⁴² and rabbit anti-PIN1 (ref. 51) polyclonal antibody diluted in blocking solution 1:600 and 1:1,000, respectively) for 2 h at 37 °C. Secondary antibody incubation was carried on for 2 h at 37 °C. Anti-rabbit-Alexa 488 (Sigma A-11034) and CY3-conjugated anti-rabbit antibody (Sigma, C2306) were diluted 1:600 in blocking solution. Control staining was done with propidium iodide diluted 1:1,000 in water. Samples were mounted in solution containing 25 mg ml⁻¹ DABCO (Sigma) in 90% glycerol, 10% PBS, pH 8.5. Expression was monitored using a confocal laser scanning microscope (LSM 510, Zeiss). Images were analysed by using ImageJ software.

Confocal imaging and image analysis. Zeiss LSM 510, Zeiss LSM 710 or Olympus FV10 ASW confocal scanning microscopes using either $\times 20$ or $\times 60$ (water immersion) objectives were employed to monitor expression of fluorescent reporters. GFP and propidium iodide signals were detected either at 488 nm excitation/507 nm emission or 536 nm excitation/617 nm emission wavelength, respectively. For real-time analysis of PIN7-GFP expression in LRP, 6-day-old seedlings were placed on chambered cover glass (Nunc Lab-Tek) and covered with 0.2-mm-thin square blocks of solid 0.5 \times MS media with or without cytokinin. LRPs were scanned in 30-min time intervals for 16 h by the FV10 ASW confocal microscope (Olympus). To evaluate relative PIN7-GFP expression levels, a minimum of 10 LRPs in stage-I positioned in the plane with two xylem strands were selected, and the PIN-GFP membrane signals at two anticlinal plasma membranes per LRP were measured. Quantification of PIN-GFP or immunodetected PIN expression in root meristems was performed by measurement of membrane signal in either pericycle or endodermal cells ($n = 10$ roots, five cells per root) using ImageJ. About 10–15 seedlings were analysed, the statistical significance was evaluated by Student's *t*-test.

Auxin accumulation in root tips of *crf3crf6* double mutants. Root tips (2-mm segments, about 100 mg) of 6-day-old *A. thaliana* (L.) Heynh. seedlings grown on vertical plates were separated and collected in 300 µl Bieleckis solution and homogenized. After overnight extraction at -20 °C, the tissues were separated by centrifugation (15,000g) and extracts were evaporated to dryness. Quantification of auxin and auxin metabolites was performed by HPLC-MS/MS according to ref. 52, in short: dried samples were dissolved in 50 µl 10% (v/v) acetonitrile in water and centrifuged (15,000g, 10 min, 4 °C). An aliquot (10 µl) of each supernatant was separately applied to HPLC (Ultimate 3000, Dionex) coupled to a hybrid triple quadrupole/linear ion trap mass spectrometer (3200 Q TRAP, Applied Biosystems). Calibration was performed using a multilevel calibration graph with (2H)-labelled internal standards. Results represent the mean of three independent repeats for each sample.

Y1H screen. The yeast strain YMA271 and destination vectors *pDEST-MW1* and *pDEST-MW2* have been previously described⁵³. Yeast reporter strains were designed as described⁵³. For the Y1H cDNA library screen, the 200-bp promoter fragments *PCRE1* and *PCRE7* were cloned into the destination vectors *pDEST-MW1* and *pDEST-MW2*, respectively, by Gateway cloning (for primers sequences see Supplementary Table 2). The DNA baits were integrated into yeast using the high efficiency transformation protocol according to the Yeast Protocol Handbook (Clontech) except that 1 µg of linearized plasmid DNA was added to the competent yeast, the heat shock period at 42 °C was extended to 20 min and the cells were resuspended in 150 µl TE buffer. The cDNA Y1H library screen was performed with a REGIA and REGULATORS (RR) collection, previously described²². For the transformation of one TF, 20 µl of competent yeast, 2 µl of carrier DNA, 100 ng plasmid (TF) DNA and 100 µl of TE/LiAC/PEG were used. Yeast cells were resuspended in 20 µl TE buffer and spotted on SD-His-Ura-Trp medium. After 3 days of growing, replica plates were made with 0, 15 and 30 mM 3-aminotriazole and positive clones were selected after 6 to 8 days of incubation at 30 °C.

Transient expression in *Arabidopsis* mesophyll protoplasts. Mesophyll protoplasts were isolated from rosette leaves of 4-week-old *Arabidopsis* plants grown in soil under controlled environmental conditions in a 16:8 h light/dark cycle or under continuous light at 21 °C. Protoplasts were isolated and transient expression assays were carried out as described⁵⁴ with modifications⁵⁵. Protoplasts were co-transfected with 20 µg of a reporter plasmid that contained *lUC*, a reporter gene driven by the corresponding promoter, 2 µg of normalization plasmid expressing the *Renilla LUC* (*rLUC*) under the control of the 35S promoter and 20 µg of the effector construct. For the reporter constructs, the *pEN-L4-Pro-R1* vector (with Pro representing *PIN1::LUC*, $\Delta PIN1::LUC$, *PIN7::LUC*, and $\Delta PIN7::LUC$) was recombined together with *pEN-L1- β -GLUC-L2* by Multisite Gateway LR cloning with *pm42GW736*. For the effector constructs, the *pEN-L1-ORF-R2* plasmids (with the ORF of *CRF2*, *CRF3* or *CRF6*) were used to introduce the ORFs by Gateway LR cloning into *p2GW7* for overexpression.

The total amount of DNA was equalized in each experiment with the *p2GW7-GUS* mock effector plasmid. After transfection, protoplasts were incubated overnight and then lysed; *lUC* and *rLUC* activities were determined with the

Dual-Luciferase reporter assay system (Promega). Variations in transfection efficiency and technical errors were corrected by normalization of fLUC by the eLUC activities. The mean value was calculated from three measurements and each experiment was repeated at least three times.

Transient expression in root suspension culture protoplasts. The LUC assays were performed from 3-days-old *Arabidopsis* root suspension culture by PEG mediated transformation. Protoplasts were isolated in enzyme solution (1% cellulose-Yakult, 0.2% Macerozyme; Yakult in B5-0.34M glucose-mannitol solution; 2.2 g MS with vitamins, 15.25 g glucose, 15.25 g mannitol, H₂O to 500 ml pH to 5.5 with KOH) with slight shaking for 3–4 h, centrifuged at 800g for 5 min. The pellet was washed with B5-0.34M glucose-mannitol solution and resuspended in B5-0.34M glucose-mannitol solution to a final concentration of 2×10^5 per 50 μ l. 2 μ g of reporter and effector plasmid DNAs were gently mixed together with 50 μ l of protoplast suspension and 60 μ l of PEG solution (0.1 M Ca(NO₃)₂, 0.45 M Mannitol, 25% PEG 6000) and incubated in the dark for 10 min. Then 140 μ l of 0.275 M Ca(NO₃)₂ solution was added to wash off PEG, centrifuged at 800g for 5 min and supernatant was removed. The protoplast pellet was resuspended in 200 μ l of B5-0.34M glucose-mannitol solution and incubated for 16 h in the dark at room temperature. The LUC assays were performed using a Dual-Luciferase Reporter Assay System as described for mesophyll protoplasts above. For cloning of the *PIN2wt:LUC* construct, 1.5 kb fragment of the *PIN2* promoter upstream from the translational start was PCR amplified from the genomic DNA using Sall-Fw and NcoI-Rv primers and the PCR product was subsequently cloned as Sall + NcoI fragment into the pGreen008-II-Luc vector⁵⁶ in frame with the coding sequence of the *LUC* gene.

For introducing *PCRE7* motives, mutagenesis by PCR-driven overlap extension technique was used as described previously in ref. 57. Briefly, intermediate primers containing *PCRE7* motives were designed with complementary ends and PCRs were performed using following primer combinations (listed in Supplementary Table 1): For introducing *PCRE7-1* motif, Sall-Fw primer in combination with *PCRE7-1-Rv* and NcoI-Rv primer in combination with *PCRE7-1-Fw* were used, and *PIN2wt* promoter DNA was used as template. The two PCRs products were purified and combined in equal concentrations and were subsequently used as template in the extension PCR round to get a full length *PIN2* promoter with *PCRE7-1* motif. Similarly for introducing *PCRE7-3*, Sall-Fw primer in combination with *PCRE7-3-Rv* and NcoI-Rv primer in combination with *PCRE7-3-Fw* were used, in this case and *PIN2* promoter with *PCRE7-1* motif was used as template. The two PCRs products were purified and combined in equal concentrations and were subsequently used as template in the extension PCR round to get a full length *PIN2* promoter with *PCRE7-3* motif. The PCR products were subsequently cloned into as Sall + NcoI fragment into the pGreen008-II-Luc vector.

ChIP assay. ChIP experiments were done as described⁵⁸ with minor modifications. One gram of tissue from 8-day-old plants was harvested and immersed in 1% formaldehyde under vacuum for 10 min. Glycine was added to a final concentration of 0.125 M and incubation was continued for 5 min. After washing, the nuclei were isolated and cross-linked DNA/protein complexes were fragmented by sonication with a Bioruptor sonicator (Diagenode), resulting in fragments of ~500 bp. After centrifugation (at 500g), the supernatant was precleared with 80 μ l of sheared salmon sperm DNA and protein A agarose (Millipore), of which 10 μ l was used as input and the remainder was divided into three samples. To two samples (IP1 and IP2), 25 μ l GFP-Trap_A coupled to agarose beads (Chromotec, gta-20) was added, whereas to the third sample, which served as IgG control, an equal volume of nonspecific control serum was added, consisting of sonicated salmon sperm DNA, BSA and protein A (salmon sperm DNA/protein A agarose-50% slurry). The samples were incubated overnight and immunoprecipitates were subsequently eluted from the beads. All centrifugation steps with bead-containing samples were done at 500g. Proteins were de-cross-linked and DNA was purified by phenol/chloroform/isoamyl alcohol extraction and ethanol precipitation. Pellets were resuspended in MiliQ water. The concentration of ChIP DNA was measured with the Quant-iT double-stranded DNA HS assay kit (Invitrogen). The SYBR Green I Master kit was used for all qPCRs. *ACTIN2* and promoter regions of *PIN1* (433–512 bp upstream of the start codon) and *PIN7* (357–553 upstream of the ATG) were utilized as negative controls. All primer sequences, including those for *PCRE1* and *PCRE7*, as well as primers used for identification of CRF motif are listed in Supplementary Table 2. To analyse the ChIP enrichment from qPCR data, the Percent Input Method and Fold Enrichment Method were used.

Each ChIP DNA fractions' Ct value was normalized to the Input DNA fraction Ct value for the same qPCR Assay (Δ Ct). Δ Ct [normalized ChIP] = (Ct [ChIP] – (Ct [Input] – Log₂ (Input Dilution Factor))). In which Input Dilution Factor (Fd) = 1/100 (fraction of the input chromatin saved). The average of normalized ChIP Ct values for replicate samples was calculated. Percent Input was then calculated as: %input = $2^{-(\Delta$ Ct (normalized ChIP))}. The normalized ChIP fraction Ct value was adjusted for the normalized background (IgG) fraction Ct value (first Δ ΔCt). Δ ΔCt (ChIP/IgG) = Δ Ct (normalized ChIP) – Δ Ct (normalized IgG). IP Fold Enrichment above the sample specific background was calculated as linear conversion of the first Δ ΔCt: Fold Enrichment = $2^{-(\Delta$ ΔCt (ChIP/IgG))}. S.d. was calculated for IP1 and IP2 as $\ln(2) \times \text{dSD} \times \text{FC}$ and for IgG as $\ln(2) \times \text{dSD}$,

with FC the fold change. ChIP data were obtained from single experiments, but similar data were acquired from three independent experiments.

References

- Friml, J. *et al.* Efflux-dependent auxin gradients establish the apical-basal axis of *Arabidopsis*. *Nature* **426**, 147–153 (2003).
- Müller, B. & Sheen, J. Cytokinin and auxin interaction in root stem-cell specification during early embryogenesis. *Nature* **453**, 1094–1097 (2008).
- Benková, E. *et al.* Local, efflux-dependent auxin gradients as a common module for plant organ formation. *Cell* **115**, 591–602 (2003).
- Bielach, A. *et al.* Spatiotemporal regulation of lateral root organogenesis in *Arabidopsis* by cytokinin. *Plant Cell* **24**, 3967–3981 (2012).
- Laplace, L. *et al.* Cytokinins act directly on lateral root founder cells to inhibit root initiation. *Plant Cell* **19**, 3889–3900 (2007).
- Leyser, O. The control of shoot branching: an example of plant information processing. *Plant Cell Environ.* **32**, 694–703 (2009).
- Reinhardt, D. *et al.* Regulation of phyllotaxis by polar auxin transport. *Nature* **426**, 255–260 (2003).
- Zhao, Z. *et al.* Hormonal control of the shoot stem-cell niche. *Nature* **465**, 1089–1092 (2010).
- Yoshida, S., Mandel, T. & Kuhlemeier, C. Stem cell activation by light guides plant organogenesis. *Genes Dev.* **25**, 1439–1450 (2011).
- Dello Ioio, R. *et al.* A genetic framework for the control of cell division and differentiation in the root meristem. *Science* **322**, 1380–1384 (2008).
- Růžicka, K. *et al.* Cytokinin regulates root meristem activity via modulation of the polar auxin transport. *Proc. Natl. Acad. Sci. USA* **106**, 4284–4289 (2009).
- Bishopp, A. *et al.* A mutually inhibitory interaction between auxin and cytokinin specifies vascular pattern in roots. *Curr. Biol.* **21**, 917–926 (2011).
- Hejác, J. *et al.* The histidine kinases cytokinin-independent1 and *arabidopsis* histidine kinase2 and 3 regulate vascular tissue development in *Arabidopsis* shoots. *Plant Cell* **21**, 2008–2021 (2009).
- Dharmasiri, N. *et al.* Plant development is regulated by a family of auxin receptor F box proteins. *Dev. Cell* **9**, 109–119 (2005).
- Hwang, I. & Sheen, J. Two-component circuitry in *Arabidopsis* cytokinin signal transduction. *Nature* **413**, 383–389 (2001).
- Inoue, T. *et al.* Identification of CRE1 as a cytokinin receptor from *Arabidopsis*. *Nature* **409**, 1060–1063 (2001).
- Kepinski, S. & Leyser, O. The *Arabidopsis* F-box protein TIR1 is an auxin receptor. *Nature* **435**, 446–451 (2005).
- Jones, B. *et al.* Cytokinin regulation of auxin synthesis in *Arabidopsis* involves a homeostatic feedback loop regulated via auxin and cytokinin signal transduction. *Plant Cell* **22**, 2956–2969 (2010).
- Marhavý, P. *et al.* Cytokinin modulates endocytic trafficking of PIN1 auxin efflux carrier to control plant organogenesis. *Dev. Cell* **21**, 796–804 (2011).
- Pernisová, M. *et al.* Cytokinins modulate auxin-induced organogenesis in plants via regulation of the auxin efflux. *Proc. Natl. Acad. Sci. USA* **106**, 3609–3614 (2009).
- Rashotte, A. M. *et al.* A subset of *Arabidopsis* AP2 transcription factors mediates cytokinin responses in concert with a two-component pathway. *Proc. Natl. Acad. Sci. USA* **103**, 11081–11085 (2006).
- Castrillo, G. *et al.* Speeding cis-trans regulation discovery by phylogenomic analyses coupled with screenings of an arrayed library of *Arabidopsis* transcription factors. *PLoS ONE* **6**, e21524 (2011).
- Lu, G. & Moriyama, E. N. Vector NTI, a balanced all-in-one sequence analysis suite. *Brief. Bioinform.* **5**, 378–388 (2004).
- Fujimoto, S. Y., Ohta, M., Usui, A., Shinshi, H. & Ohme-Takagi, M. *Arabidopsis* ethylene-responsive element binding factors act as transcriptional activators or repressors of GCC box-mediated gene expression. *Plant Cell* **12**, 393–404 (2000).
- Weirauch, M. T. *et al.* Determination and inference of eukaryotic transcription factor sequence specificity. *Cell* **158**, 1431–1443 (2015).
- Hao, D., Yamasaki, K., Sarai, A. & Ohme-Takagi, M. Determinants in the sequence specific binding of two plant transcription factors, CBF1 and NTERF2, to the DRE and GCC motifs. *Biochemistry* **41**, 4202–4208 (2002).
- Hall, D. B., Wade, J. T. & Struhl, K. An HMG protein, Hmo1, associates with promoters of many ribosomal protein genes and throughout the rRNA gene locus in *Saccharomyces cerevisiae*. *Mol. Cell. Biol.* **26**, 3672–3679 (2006).
- Růžicka, K. *et al.* *Arabidopsis* PIS1 encodes the ABCG37 transporter of auxinic compounds including the auxin precursor indole-3-butyric acid. *Proc. Natl. Acad. Sci. USA* **107**, 10749–10753 (2010).
- Zwack, P. J., Robinson, B. R., Risley, M. G. & Rashotte, A. M. Cytokinin Response Factor 6 negatively regulates leaf senescence and is induced in response to cytokinin and numerous abiotic stresses. *Plant Cell Physiol.* **54**, 971–981 (2013).
- Cutcliffe, J. W., Hellmann, E., Heyl, A. & Rashotte, A. M. CRFs form protein-protein interactions with each other and with members of the cytokinin signalling pathway in *Arabidopsis* via the CRF domain. *J. Exp. Bot.* **62**, 4995–5002 (2011).

31. Friml, J. *et al.* AtPIN4 mediates sink-driven auxin gradients and root patterning in *Arabidopsis*. *Cell* **108**, 661–673 (2002).
32. Bilou, I. *et al.* The PIN auxin efflux facilitator network controls growth and patterning in *Arabidopsis* roots. *Nature* **433**, 39–44 (2005).
33. Laskowski, M. *et al.* Root system architecture from coupling cell shape to auxin transport. *PLoS Biol.* **6**, e307 (2008).
34. Cary, A. J., Liu, W. & Howell, S. H. Cytokinin action is coupled to ethylene in its effects on the inhibition of root and hypocotyl elongation in *Arabidopsis thaliana* seedlings. *Plant Physiol.* **107**, 1075–1082 (1995).
35. Dello Ioio, R. *et al.* Cytokinins determine *Arabidopsis* root-meristem size by controlling cell differentiation. *Curr. Biol.* **17**, 678–682 (2007).
36. Abas, L. *et al.* Intracellular trafficking and proteolysis of the *Arabidopsis* auxin-efflux facilitator PIN2 are involved in root gravitropism. *Nat. Cell Biol.* **8**, 249–256 (2006).
37. Ding, Z. *et al.* Light-mediated polarization of the PIN3 auxin transporter for the phototropic response in *Arabidopsis*. *Nat. Cell Biol.* **13**, 447–452 (2011).
38. Swarup, R. *et al.* Ethylene upregulates auxin biosynthesis in *Arabidopsis* seedlings to enhance inhibition of root cell elongation. *Plant Cell* **19**, 2186–2196 (2007).
39. Willige, B. C., Isono, E., Richter, R., Zourelidou, M. & Schwechheimer, C. Gibberellin regulates PIN-FORMED abundance and is required for auxin transport-dependent growth and development in *Arabidopsis thaliana*. *Plant Cell* **23**, 2184–2195 (2011).
40. Zwack, P. J. *et al.* Vascular expression and C-terminal sequence divergence of cytokinin response factors in flowering plants. *Plant Cell Physiol.* **53**, 1683–1695 (2012).
41. Scarpella, E., Marcos, D., Friml, J. & Berleth, T. Control of leaf vascular patterning by polar auxin transport. *Genes Dev.* **20**, 1015–1027 (2006).
42. Schlereth, A. *et al.* MONOPTEROS controls embryonic root initiation by regulating a mobile transcription factor. *Nature* **464**, 913–916 (2010).
43. Inzé, A. *et al.* A subcellular localization compendium of hydrogen peroxide-induced proteins. *Plant Cell Environ.* **35**, 308–320 (2012).
44. Sessions, A. *et al.* A high-throughput *Arabidopsis* reverse genetics system. *Plant Cell* **14**, 2985–2994 (2002).
45. Rosso, M. G. *et al.* An *Arabidopsis thaliana* T-DNA mutagenized population (GABI-Kat) for flanking sequence tag-based reverse genetics. *Plant Mol. Biol.* **53**, 247–259 (2003).
46. Karimi, M., Inzé, D. & Depicker, A. GATEWAY vectors for *Agrobacterium*-mediated plant transformation. *Trends Plant Sci.* **7**, 193–195 (2002).
47. Karimi, M., Depicker, A. & Hilson, P. Recombinational cloning with plant Gateway vectors. *Plant Physiol.* **145**, 1144–1154 (2007).
48. Clough, S. J. & Bent, A. F. Floral dip: a simplified method for *Agrobacterium*-mediated transformation of *Arabidopsis thaliana*. *Plant J.* **16**, 735–743 (1998).
49. Malamy, J. E. & Benfey, P. N. Organisation and cell differentiation in lateral roots of *Arabidopsis thaliana*. *Development* **124**, 33–44 (1997).
50. Sauer, M., Paciorek, T., Benková, E. & Friml, J. Immunocytochemical techniques for whole-mount *in situ* protein localization in plants. *Nat. Protoc.* **1**, 98–103 (2006).
51. Paciorek, T. *et al.* Auxin inhibits endocytosis and promotes its own efflux from cells. *Nature* **435**, 1251–1256 (2005).
52. Dobrev, P. & Vankova, R. In: *Plant Salt Tolerance: Methods and Protocols, Methods in Molecular Biology*. (eds Shabala, S. & Cuin, T. A.) **913**, 251–261 (Humana Press (2012)).
53. Deplancke, B., Dupuy, D., Vidal, M. & Walhout, A. J. M. A gateway-compatible yeast one-hybrid system. *Genome Res.* **14**, 2093–2101 (2004).
54. Wu, F.-H. *et al.* Tape-*Arabidopsis* Sandwich—a simpler *Arabidopsis* protoplast isolation method. *Plant Methods* **5**, 16 (2009).
55. Wehner, N. *et al.* High-throughput protoplast transactivation (PTA) system for the analysis of *Arabidopsis* transcription factor function. *Plant J.* **68**, 560–569 (2011).
56. Hellens, R. P. *et al.* Transient expression vectors for functional genomics, quantification of promoter activity and RNA silencing in plants. *Plant Methods* **1**, 13 (2005).
57. Heckman, K. L. & Pease, L. R. Gene splicing and mutagenesis by PCR-driven overlap extension. *Nat. Protoc.* **2**, 924–932 (2007).
58. Bowler, C. *et al.* Chromatin techniques for plant cells. *Plant J.* **39**, 776–789 (2004).

Acknowledgements

We thank Dr L. De Veylder for sharing yeast strain and vectors; professor J. Kieber and Dr A. Rashotte for sharing material; Dr B. Berckmans, F. De Winter, Dr B. Parizot for technical advice and Dr A. Bleys for help in preparing the manuscript. This work was supported by the European Research Council Starting Independent Research grant (ERC-2007-Stg-207362-HCPO to E.B., M.S., C.C.), by the Ghent University Multidisciplinary Research Partnership ‘Biotechnology for a Sustainable Economy’ no.01MRB510W, by the Research Foundation—Flanders (grant 3G033711 to J.-A.O.), by the Austrian Science Fund (FWF01_I1774S) to K.Ö., E.B., and by the Interuniversity Attraction Poles Programme (IUAP P7/29 ‘MARS’) initiated by the Belgian Science Policy Office. I.D.C. and S.V. are post-doctoral fellows of the Research Foundation—Flanders (FWO). This research was supported by the Scientific Service Units (SSU) of IST-Austria through resources provided by the Bioimaging Facility (BIF), the Life Science Facility (LSF).

Author contributions

E.B., M.Š. and J.A.B. designed the research; M.Š., J.A.B. and M.K. conducted most experiments; K.H. and A.M. performed auxin measurements; M.Š., I.D.C. and K.Ö. performed ChIP assay; M.Š., C.C. and M.K. performed transient expression assay in protoplasts; M.Š., I.D.C. and F.B. performed yeast 1-hybrid assay; P.M. performed lateral root expression analysis; K.W. performed *in silico* promoter analyses; J.M.A.V.H., G.V.N., A.V., S.V., F.V.B., D.W., M.N., T.B. and J.F., shared unpublished material. M.Š. and E.B. wrote the paper. All authors discussed the results and collectively edited the manuscript.

Additional information

Supplementary Information accompanies this paper at <http://www.nature.com/naturecommunications>

Competing financial interests: The authors declare no competing financial interests.

Reprints and permission information is available online at <http://npg.nature.com/reprintsandpermissions/>

How to cite this article: Šimášková, M. *et al.* Cytokinin response factors regulate PIN-FORMED auxin transporters. *Nat. Commun.* 6:8717 doi: 10.1038/ncomms9717 (2015).